

Gain dynamics in a CO₂ active medium optically pumped at 4.3 μm

Cite as: J. Appl. Phys. **128**, 103103 (2020); <https://doi.org/10.1063/5.0014020>

Submitted: 15 May 2020 . Accepted: 31 July 2020 . Published Online: 09 September 2020

 D. Tovey, J. J. Pigeon,  S. Ya. Tochitsky, G. Louwrens, I. Ben-Zvi,  C. Joshi, D. Martyshkin, V. Fedorov, K. Karki, and  S. Mirov



View Online



Export Citation



CrossMark

ARTICLES YOU MAY BE INTERESTED IN

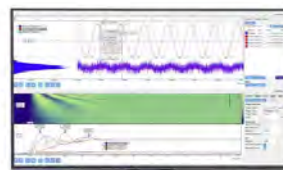
[Charge carrier spatial distribution effects in photomodulated reflectivity of 4H-SiC and GaN](#)
Journal of Applied Physics **128**, 103102 (2020); <https://doi.org/10.1063/5.0017579>

[Point defects in two-dimensional hexagonal boron nitride: A perspective](#)
Journal of Applied Physics **128**, 100902 (2020); <https://doi.org/10.1063/5.0021093>

[Anisotropic properties of monolayer 2D materials: An overview from the C2DB database](#)
Journal of Applied Physics **128**, 105101 (2020); <https://doi.org/10.1063/5.0021237>

Challenge us.

What are your needs for periodic signal detection?



Zurich Instruments



Gain dynamics in a CO₂ active medium optically pumped at 4.3 μm

Cite as: J. Appl. Phys. 128, 103103 (2020); doi: 10.1063/5.0014020

Submitted: 15 May 2020 · Accepted: 31 July 2020 ·

Published Online: 9 September 2020



D. Tovey,^{1,a)} J. J. Pigeon,² S. Ya. Tochitsky,^{1,b)} G. Louwrens,¹ I. Ben-Zvi,² C. Joshi,¹ D. Martyshkin,³ V. Fedorov,³ K. Karki,³ and S. Mirov³

AFFILIATIONS

¹Department of Electrical Engineering, University of California at Los Angeles, Los Angeles, California 90095, USA

²Department of Physics and Astronomy, Stony Brook University, Stony Brook, New York 11974, USA

³Department of Physics, University of Alabama at Birmingham, Birmingham, Alabama 35294, USA

^{a)}Author to whom correspondence should be addressed: danatovey@ucla.edu

^{b)}sergei12@ucla.edu

ABSTRACT

A pulsed ~2 mJ Fe:ZnSe laser tunable around ~4.3 μm is used to optically pump mixtures of CO₂ and He to create gain at 10 μm. A conventional low-pressure CO₂ laser operating on both regular (001-100) and sequence (002-101) bands is used to study the gain dynamics of the optically pumped CO₂ amplifier. Time-resolved measurements of the CO₂ asymmetric stretching mode vibrational temperature, T₃, as well as the translational temperature, T, are made. The measured T₃ value of ~2500 K is much higher than that typically measured in discharge pumped CO₂ lasers. High gain coefficients ~30%/cm in the optically pumped active medium are attributed to the efficient storage of energy in the asymmetric stretching mode and the selective population of the upper laser level. The measured optical-to-optical energy conversion efficiency of ~30% for 10 μm lasing at sub-atmospheric pressures is close to the theoretical quantum limit of 40% and, thus, supports our claim of gain dynamics optimization. It is concluded that a joule-class 4.3 μm pump laser will be required for the amplification of sub-picosecond 10 μm pulses in a multi-atmosphere optically pumped CO₂ active medium.

Published under license by AIP Publishing. <https://doi.org/10.1063/5.0014020>

I. INTRODUCTION

High peak power short pulses in the long-wave infrared (LWIR) region (8–14 μm) are of interest for strong field physics and nonlinear optics studies.^{1–3} Optical parametric chirped pulse amplification using nonlinear converters has recently become a popular technique for producing powerful pulses in the mid-infrared,^{4–6} but physical damage of the crystal and low conversion efficiencies have prevented the generation of pulses with energies greater than a few millijoules, thereby limiting the achievable peak power. A CO₂ active medium can store joules of energy, and collisional broadening at high pressures (>10 atm) results in a gain spectrum with a bandwidth sufficient for picosecond pulse amplification at ~10 μm wavelength [see Fig. 1(a)].^{7,8} Operating at the necessary pressures to achieve this bandwidth in electric discharge pumped CO₂, however, is extremely challenging due to the difficulty in maintaining a stable discharge at pressures above 10 atm across a large aperture.

Pumping the CO₂ molecule optically removes this pressure limitation and, thus, may offer a more efficient path toward generating sub-picosecond pulses in the LWIR than these currently existing technologies. Short pulse amplification has never been demonstrated in an optically pumped CO₂ active medium, but our recent numerical study indicates that a high pressure optically pumped CO₂ isotopic mixture is capable of amplifying 10 μm pulses shorter than 1 ps.⁹ This concept has not been thoroughly pursued experimentally primarily due to the lack of an energetic pump source at ~4.3 μm, corresponding to the channel by which population can be moved directly from the ground state to the upper laser levels of the 10 μm transitions in CO₂ [see Fig. 1(b)]. The use of HBr chemical lasers constrained pumping schemes to the coincidental overlap between available laser lines and the CO₂ absorption spectrum, and 4.3 μm CO₂ lasers lack sufficient energy to be used as an efficient pump for high-power CO₂ laser technology.^{10–12} The recent development of tunable solid-state

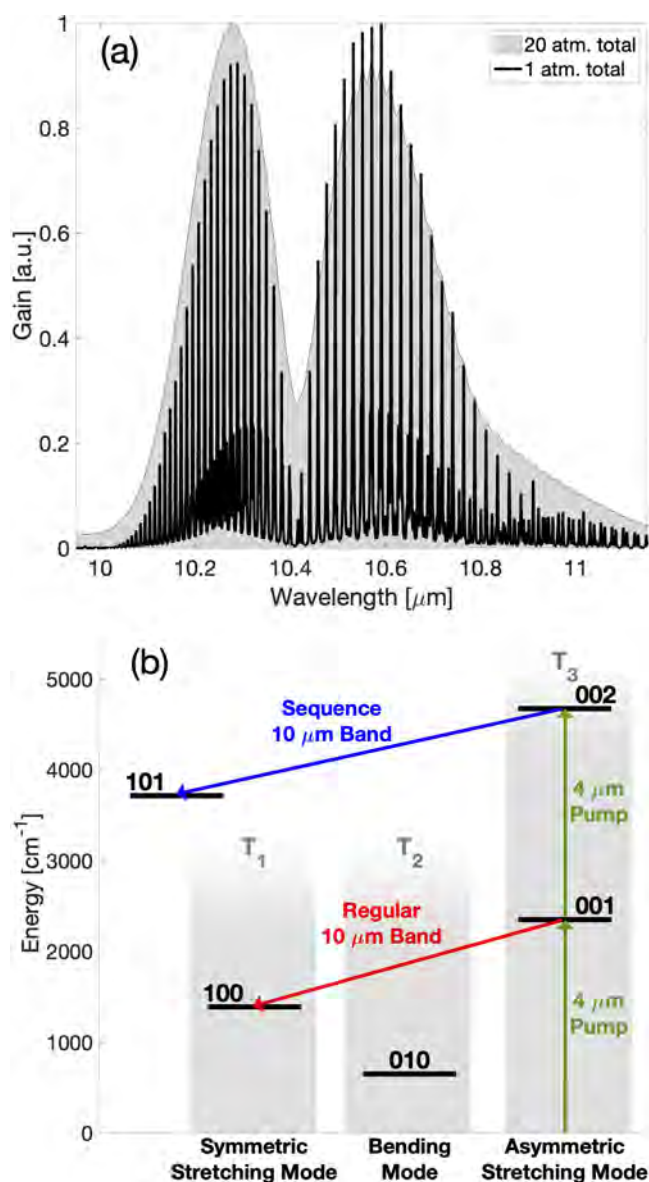


FIG. 1. (a) The normalized gain spectrum in a 1:19 CO₂:He active medium at total pressures of 1 atm (black) and 20 atm (gray). (b) A simplified energy band diagram showing relevant vibrational energy levels for the CO₂ molecule. The three different vibrational modes of the CO₂ molecule are represented with columns as labeled. The 4.3 μm transitions through which CO₂ can be excited are shown in green, the regular 10 μm lasing band is shown in red, and the first sequence 10 μm lasing band is shown in blue.

lasers in the mid-IR using transition metal-doped chalcogenides has provided an energetic pump source in the 4–5 μm region¹³ and opened an opportunity for testing this concept for 10 μm pulse generation. However, further progress in the development of optically pumped CO₂ lasers depends on gaining a detailed

understanding of gain dynamics in such an optically excited molecular active medium.

The properties of the discharge pumped CO₂ gain medium have been well characterized using a generally accepted temperature model in which each vibrational mode is assigned a vibrational temperature describing the Boltzmann distribution of population in that mode.^{14–16} For a CO₂ amplifier, the mode temperature of greatest interest is that of the asymmetric stretching mode, T_3 , as it describes the population of the upper laser level of interest, 001 [see Fig. 1(b)]. This temperature can be determined experimentally with measurement of the gain coefficient on both a regular band (001-100) and sequence band (002-101) transition.^{15,16} Knowledge of temperature kinetics is critical for laser optimization, and experimentally observed molecular kinetics in CO₂ lasers have been shown to deviate considerably from theoretical modeling, especially at high levels of vibrational excitation.^{11,16} Selective optical pumping of the asymmetric stretching mode has resulted in the achievement of extremely large vibrational temperatures;¹¹ however, no detailed studies have been reported on gain limitations in a CO₂-He amplifier optically pumped around 4.3 μm.

This paper reports investigations of gain dynamics in a CO₂ amplifier (pressure ≤ 1 atm) optically pumped by a 4.3 μm Fe:ZnSe laser. Time-resolved small-signal gain measurements using both regular band (001-100) and sequence band (002-101) transitions are used to determine the dynamics of asymmetric stretching mode vibrational temperature, T_3 , and translational temperature, T , after the passage of a ~40 ns pump pulse in various CO₂-He gas mixtures. We also investigate dynamics of lasing for pressures up to 1 atm. Temperature optimization resulted in record high gain coefficients of ~30%/cm and optical-to-optical conversion efficiencies of ~30%, nearing the theoretical quantum limit, in an optically pumped CO₂ laser. These results identify the ways to reach high gain in an optically pumped CO₂ cell, an important step toward the development of a compact high-pressure gas laser capable of short pulse amplification.

II. THEORY

It is known that the kinetics of the excited CO₂ molecule can be accurately described using a mode-temperature model.^{14–18} This model is derived from the relationship between relaxation times describing the primary kinetic processes occurring in molecular gases,

$$\tau_{VR} \ll \tau_{VV} \ll \tau_{VV'}, \quad (1)$$

where τ_{VR} , τ_{VV} , and $\tau_{VV'}$ are time constants describing the rates at which equilibrium is achieved among rotational energy levels, among vibrational energy levels within a single vibrational mode, and among different vibrational modes of the CO₂ molecule, respectively. Equilibrium is reached among individual rotational levels first—such that the population among these levels can be described according to a Boltzmann distribution with translational or gas temperature, T —on a time scale of $\tau_{VR} \approx 0.2$ ns at 1 atm of pressure. The distribution of population within the different vibrational energy levels in a single vibrational mode reaches a Boltzmann distribution on a time scale of $\tau_{VV} \approx 5$ ns at 1 atm. Equilibrium among different vibrational modes or different gases (e.g., N₂) within a mixture occurs on a much longer time scale of $\tau_{VV'} \leq 1$ μs at 1 atm. This hierarchy of relaxation times

in the CO₂ molecule is the main reason for the applicability of this temperature model when considering a typical 100 ns long pump laser pulse. The population of each vibrational energy level is, thus, best described using a Boltzmann distribution with a different temperature, T_i , assigned to each vibrational mode i ,

$$N_\nu = N_0 \exp\left(-\frac{h\nu G_i}{k_B T_i}\right), \quad (2)$$

where N_ν is the population of molecules in level ν of the mode, N_0 is the population of molecules in the ground state, G_i is the energy gap between levels in vibrational mode i , and h , c , and k_B are the usual physical constants.

The CO₂ molecule has three vibrational modes: symmetric stretching (T_1), bending (T_2), and asymmetric stretching (T_3). Figure 1(b) shows the vibrational energy levels of interest in a CO₂ laser with each column corresponding to a distinct vibrational mode. It can be seen that the upper laser levels for 10 μ m lasing transitions in CO₂ are energy states corresponding to excitation of the asymmetric stretching mode. As a result, optimizing gain in a CO₂ active medium corresponds to maximizing T_3 without increasing T_1 and T_2 . In the case of optical pumping, it is reasonable to assume that all of the absorbed pump energy is stored in this asymmetric stretching mode, while the vibrational temperatures of other modes, T_1 and T_2 , tend to be equal to the translational temperature of the gas T . As a result, optimization of gain is easier to achieve in an optically pumped CO₂ active medium than in discharge-excited CO₂ systems.¹⁶ This ability to exclusively excite the asymmetric stretching mode via the absorption of 4.3 μ m pump photons is an additional advantage of pumping CO₂ optically.

For optical excitation, the population of molecules at each individual energy level, and consequently the gain coefficients for each 10 μ m CO₂ transition, can be determined with knowledge of the vibrational temperature T_3 and translational temperature T . It is, thus, desirable to make time-resolved measurements of both T_3 and T in optically pumped CO₂ to characterize gain dynamics occurring in such a medium. The asymmetric stretching mode temperature T_3 can be calculated from measurements of small signal gain on both a regular band transition and a sequence band transition using the following relation^{11,15}:

$$\frac{g_{\text{seq}}}{g_{\text{reg}}} = 2 \exp\left(-\frac{h\nu G_3}{k_B T_3}\right), \quad (3)$$

which gives

$$T_3 = \frac{h\nu G_3}{k_B \ln\left(\frac{2g_{\text{reg}}}{g_{\text{seq}}}\right)}, \quad (4)$$

where g_{seq} is the small signal gain on a sequence band transition (002-101) and g_{reg} is the small signal gain on a regular band transition (001-100) with an equivalent rotational quantum number j . The translational temperature, T , can be calculated from measurements of small signal gain on multiple different regular band transitions. Figure 2 shows the envelope of the 10P branch of the

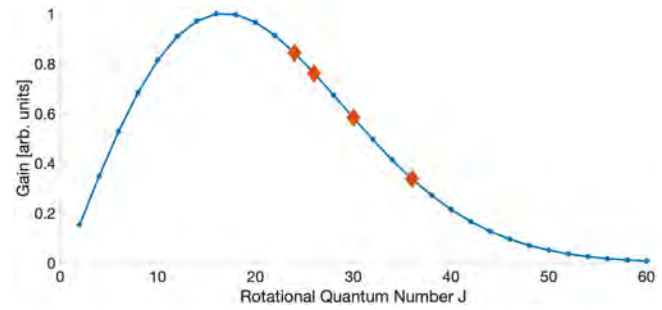


FIG. 2. The gain envelope of the regular 10 μ m branch of CO₂ transitions at a translational temperature of 300 K. The relative gain coefficient is plotted as a function of rotational quantum number J using formula (2) with $T = 300$. The rovibrational lines on which small signal gain was measured for the study detailed in this paper—10P(24), 10P(26), 10P(30), and 10P(36)—are marked with red diamonds.

normalized CO₂ gain spectrum as a function of rotational quantum number j . The shape of this envelope depends on the translational temperature T since the population of molecules in a particular rotational-vibrational state νj is given by¹⁴

$$N_{\nu j} = N_\nu \left(\frac{2hcB_\nu}{k_B T}\right) (2j+1) \exp\left(-\frac{hc}{k_B T} [B_\nu j(j+1) - D_\nu j^2(j+1)^2]\right), \quad (5)$$

where ν refers to the specific vibrational state (for example, 001), N_ν is the population of molecules in the vibrational state as a whole [given in Eq. (2)], B_ν and D_ν are rotational constants for the particular vibrational state, and j is the rotational quantum number.¹⁹ The temperature T can, thus, be found by fitting a curve to experimentally measured small-signal gain values on various 10P CO₂ transitions. The rovibrational transitions probed in this experiment are marked in Fig. 2 with red diamonds. Analysis of our method of calculating translational temperature revealed that the slope of the curve on the high- J side of the peak of the gain distribution is very sensitive to changes in temperature, so the 10P(24), 10P(26), 10P(30), and 10P(36) rovibrational transitions were chosen for our experiment. The accidental overlap between regular band lines (001-100) and sequence band (002-101) or hot band (011-110) lines was also considered when choosing rovibrational lines as these overlaps can distort the gain envelope and introduce additional error in the measurement of T .^{11,20}

The remainder of this paper discusses the experimental realization of using these methods to make time-resolved measurements of vibrational temperature T_3 and translational temperature T in optically pumped CO₂-He mixtures.

III. EXPERIMENTAL TECHNIQUES

A. 4.3 μ m Fe:ZnSe pump laser

Figure 3(a) displays a simplified schematic for the Fe:ZnSe laser used as a pump source in our experiments. A flashlamp-pumped, Q-switched 2.9 μ m Er:YAG laser producing ~ 100 ns

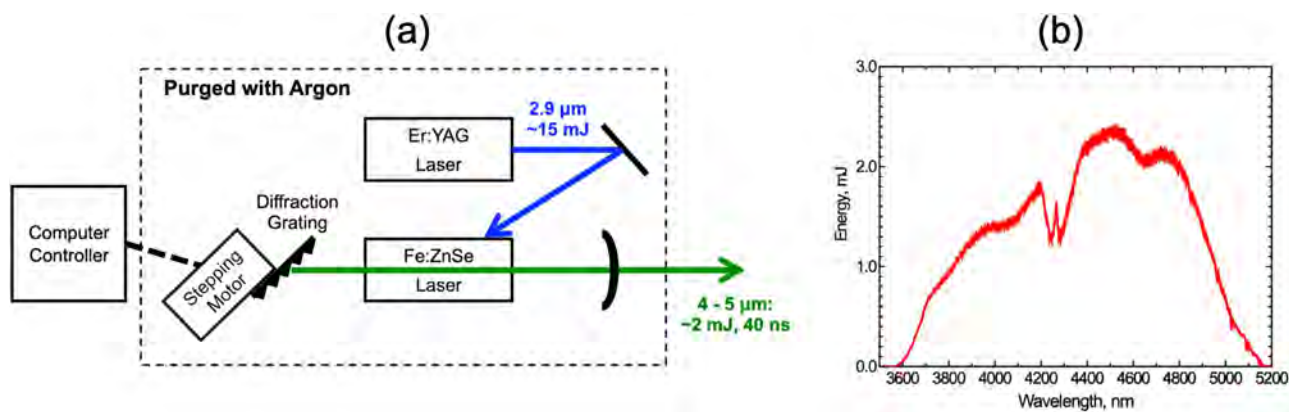


FIG. 3. (a) A simplified schematic of the tunable Fe:ZnSe pump laser. (b) Fe:ZnSe laser tuning curve. The dips in output energy at $\sim 4.3 \mu\text{m}$ are a result of absorption of CO_2 in air.

pulses of $\sim 15 \text{ mJ}$ of energy is used to pump the Fe:ZnSe crystal.²¹ A diffraction grating within the Fe:ZnSe laser cavity allows for continuous tuning over a wavelength range of 3.6–5.1 μm . Figure 3(b) shows measurements of pulse energy as a function of output wavelength; and the dip in output energy around 4.3 μm corresponds to absorption from CO_2 in air. For our experiments, the Fe:ZnSe laser system was purged with argon to eliminate this absorption. The 4.3 μm laser pulses are $\sim 40 \text{ ns}$ long, have a bandwidth of $\sim 2 \text{ nm}$, and contain up to 2.5 mJ of energy.

B. Temperature measurements in optically pumped CO_2

Figure 4 shows the simplified experimental setup used to measure small-signal gain in an optically pumped CO_2 amplifier. The tunable Fe:ZnSe laser described in Sec. III A is used to pump a 6 cm long cell containing various CO_2 -He mixtures with NaCl windows set at the Brewster angle for 10 μm light. The 2 mJ, 4.3 μm

pump pulses are focused to a peak intensity of 15 MW/cm^2 by means of a three-lens telescope, the final lens of which is a dichroic mirror ($R = 99.5\%$ at 10 μm , $T = 99\%$ at 4.3 μm) that is used as a beam combiner for the pump and probe lasers. The dichroic mirror has a radius of curvature of 70 cm.

The 10 μm probe pulses used in this experiment are produced by a 15 cm low-pressure discharge-pumped CO_2 laser. An intracavity diffraction grating (150 g/mm) is placed in a non-Littrow configuration such that the laser pulse is doubly diffracted. The cavity length of $\sim 1 \text{ m}$ and this double passing through the diffraction grating increases dispersion to allow for precise tuning of the probe laser on individual rovibrational transitions of both the regular and sequence 10 μm branches of CO_2 .²² The zeroth-order reflection of the grating is used as an output coupler to maximize the Q-factor of the cavity. Note that even with this scheme, only sequence lines with a high rotational quantum number ($j > 21$) were observed. This is a result of the frequency separation between

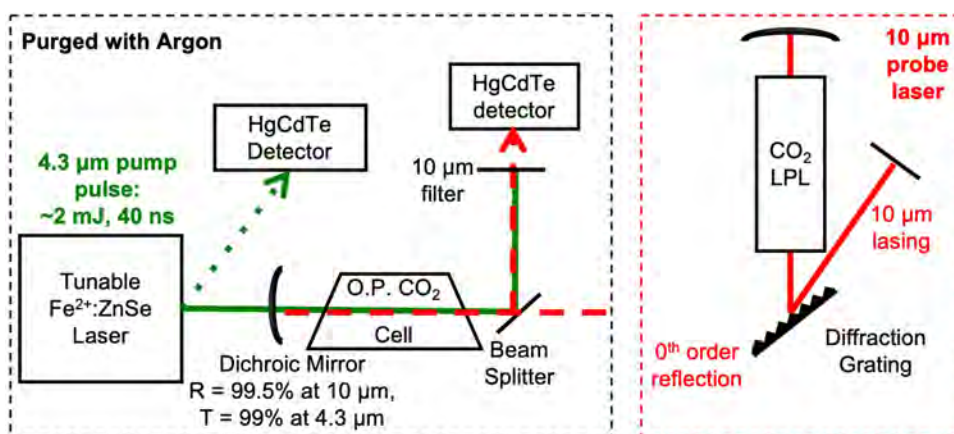


FIG. 4. The experimental setup used to measure small-signal gain in an optically pumped CO_2 active medium. OP CO_2 —optically pumped CO_2 . LPL—low pressure laser.

adjacent CO₂ regular band and sequence band transitions increasing with rotational quantum number j such that the nearby regular band transition dominates lasing within the cavity for low j sequence band transitions.

Typical regular band probe pulses contained a few mJ of energy and consisted of a short ($<1\mu\text{s}$) spike followed by a long ($>20\mu\text{s}$) tail. Measurements were performed on the tail of the pulse and the probe laser was attenuated such that the probing peak power was only a few Watts, far below gain saturation. Operation of the probe laser on sequence band transitions gave similar output with $\sim 1/3$ of the energy seen on regular band transitions. In our experiment, the 10P(23) sequence band (002-101) transition of CO₂ was used to avoid accidental overlap with hot band (011-110) lines.²⁰

The probe pulse is sent through the optically pumped CO₂ cell in a double-pass scheme with the dichroic mirror used for reflection. A 50/50 beam-splitter directs the reflected pulse into a HgCdTe signal detector for measurement. Scattered light from the 4.3 μm pump laser is measured by a HgCdTe reference detector to characterize the pump pulse. Time-resolved gain can be determined from comparison of the temporal profiles of the probe pulse and pump pulse, and, thus, time-resolved measurements of T_3 and T can be obtained using the methods described in Sec. II. It should be noted that these measurements are effective, averaged values that ignore the uneven distribution of pump energy within the cell. Given the strong absorption of 4.3 μm light by the CO₂ molecule, it is estimated that in most cases nearly all of the absorbed pump energy is deposited in the first 1–2 cm of the active medium, and the effective length over which gain is measured is significantly shorter than the full length of the cell (6 cm). Since the calculation of vibrational and translational temperatures depends only on the ratio between gain on different rovibrational transitions and not the absolute gain coefficients, precise knowledge of the gain length is not required for these temperature measurements.

IV. RESULTS AND DISCUSSION

A. Temperature measurements in optically pumped CO₂

Typical results for the measurement of small-signal gain can be seen in Fig. 5. The blue curve shows the time-resolved gain in 50 Torr of pure CO₂ pumped with ≤ 2 mJ, 4.3 μm laser pulses and probed on the 10P(24) regular band transition of CO₂. The pump wavelength was tuned to 4.29 μm , corresponding to the center of the rovibrational line at the peak of the 4R branch of the CO₂ absorption spectrum. The red curve shows the time-resolved gain of the 10P(23) sequence band transition under identical conditions. Translational temperature T and vibrational temperature T_3 are determined using these measurements and similar measurements on additional regular band transitions as described in Sec. II.

Figure 6 shows the results of these measurements for the 50 Torr pure CO₂ active medium described above. Asymmetric stretching mode vibrational temperature T_3 [see Fig. 6(a)] and translational temperature T [see Fig. 6(b)] are shown as a function of time. It can be seen that almost immediately after the absorption of the 40 ns, 4.29 μm pump pulse (at time $t = 0$), a peak T_3 value of ~ 2400 K is reached, while translational temperature is measured to be near room temperature (~ 300 K) as expected. This T_3 value corresponds to a record-high peak gain coefficient of $\sim 30\%/cm$.

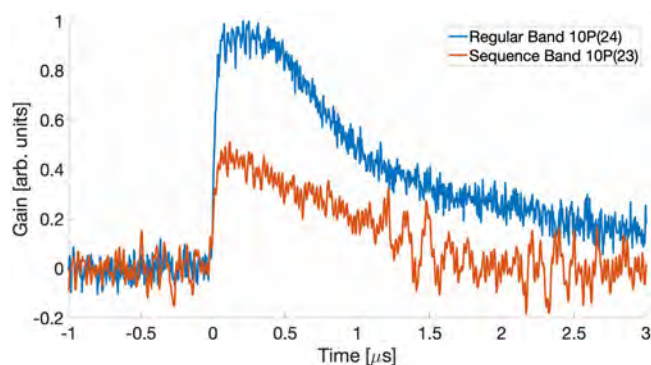


FIG. 5. Small-signal gain measurements in a 50 Torr CO₂ cell optically pumped at 4.3 μm . Gain is shown as a function of time for a regular band transition 10P(24) and a sequence band transition 10P(23).

Note that a Transversely Excited Atmospheric (TEA) CO₂ laser pumped by electric discharge rarely achieves a T_3 value above ~ 1500 K or gain coefficients above 2–3%/cm.¹⁴ Even optimized, non-self-sustained discharge-pumped CO₂ systems are typically only capable of reaching gain coefficients of 4–6%/cm. The asymmetric stretching mode then collisionally relaxes and energy is redistributed to other modes, resulting in a decrease in T_3 and an increase in gas temperature T as shown. It should be noted the observation of gain

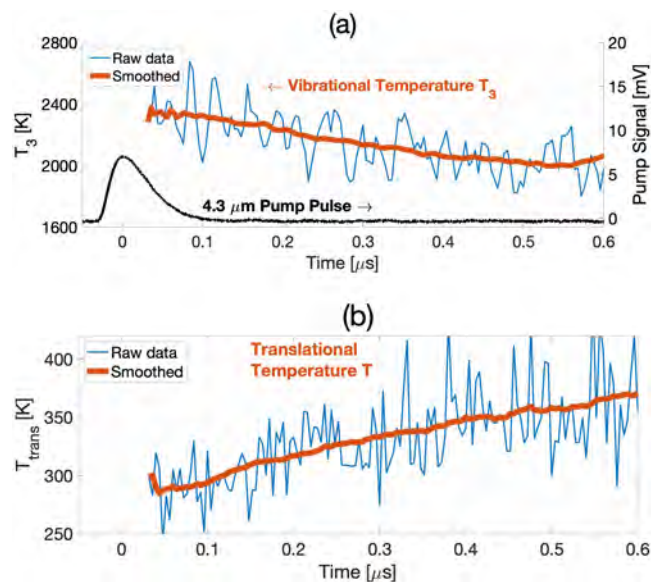


FIG. 6. (a) The asymmetric stretching mode vibrational temperature T_3 and (b) the translational temperature T within a cell of 50 Torr pure CO₂ optically pumped at 4.3 μm as a function of time. The blue curves show the results of raw data; and the red curves show these data with a 50 point moving average filter applied to reduce noise. The pump pulse temporal profile is shown in black.

on a sequence band transition (002-101) immediately after pumping gives further confirmation that the asymmetric stretching mode reaches equilibrium before the gas mixture as a whole.

These measurements were repeated for various CO₂-He mixtures to determine the effect of adjusting total pressure and CO₂ concentration on peak values of T_3 . We were only able to obtain large T_3 values in mixtures with small amounts of CO₂ gas, suggesting that a more energetic 4.3 μm pump laser is required to obtain high T_3 values in a larger partial pressure of CO₂. To study the scalability of this system to the high pressures required for sub-picosecond pulse amplification,⁹ theoretical calculations were performed to estimate the 4.3 μm pump energy required to achieve high gain in CO₂ at different pressures.

Figure 7 shows theoretical calculations for the vibrational temperature, T_3 , and the corresponding peak gain coefficient as a function of absorbed energy per unit volume for various amounts of pure CO₂ gas. The pump energy is assumed to be entirely deposited into the asymmetric stretching mode, resulting in the following equation relating T_3 and absorbed pump energy¹¹:

$$E_{abs} = \frac{N_{CO_2} \left(\sum_{v=1}^9 E_v N_v \right)}{\sum_{v=0}^9 N_v},$$

where N_{CO_2} is the total number density of CO₂ molecules, E_v is the energy of the $00v$ vibrational state, and N_v is the population of this

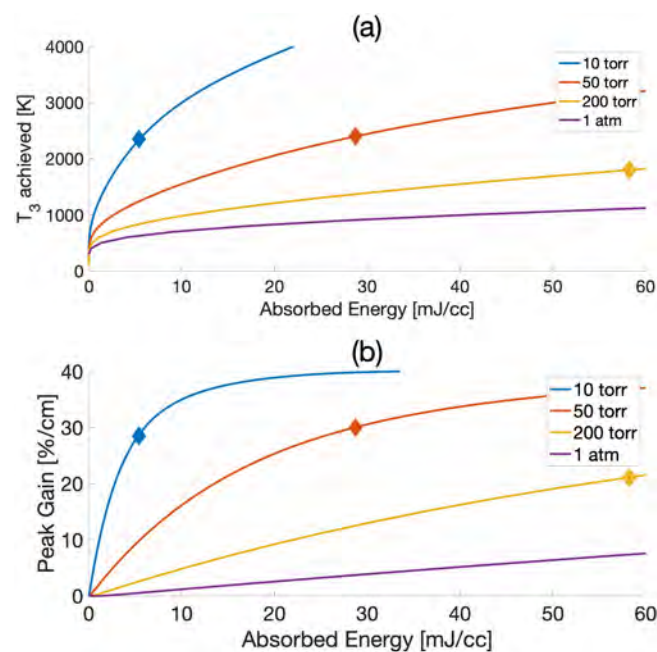


FIG. 7. (a) The asymmetric stretching vibrational mode temperature T_3 and (b) the corresponding peak gain coefficient (bottom) in an optically pumped CO₂ active medium vs absorbed 4.3 μm pump energy per volume. Each color corresponds to a different amount of pure CO₂. Experimental measurements are shown in diamonds.

state [see Eq. (2)]. The diamond markers in Fig. 7 indicate experimentally measured T_3 values and their corresponding gain coefficients. It is estimated that nearly all of the pump energy is absorbed in the cell in the 200 Torr case, corresponding to an absorbed energy per volume of ~ 60 mJ/cc. It is, thus, apparent that a much greater amount of pump energy is required to achieve $T_3 > 2000$ K in more than 50 Torr CO₂ due to simple conservation of energy. The lack of absorbed energy in the 10 Torr case is attributed to the extremely small width of the 4.3 μm CO₂ absorption spectral lines at such low pressures in comparison with the 2 nm bandwidth of the 4.3 μm pump laser.

To further investigate gain limitations in an optically pumped CO₂ system, measurements were performed in mixtures where the concentration of CO₂ is heavily diluted with helium. Figure 8 shows experimental measurements of peak T_3 as a function of pressure in pure CO₂ (the red curve) and in CO₂-He mixtures containing a constant 10 Torr of CO₂ and ballast He (the blue curve). It is clear that increasing the amount of CO₂ reduces T_3 for the reasons discussed above. It is also evident, however, that increasing the amount of helium while maintaining constant partial pressure of CO₂ increases T_3 . This result is attributed to increased absorption of 4.3 μm pump energy due to the broadening of spectral lines via CO₂-He collisions. These results give further evidence that very high vibrational temperatures ($T_3 \leq 4000$ K) can be achieved in a CO₂ system optically pumped by Fe:ZnSe laser pulses but a multi-atmosphere CO₂ laser will require a much more energetic pump source.

Small-signal gain measurements were also used to estimate gain lifetime at low pressures. Using the inverse linear relationship between upper state lifetime and total pressure, it is estimated that for total pressures approaching 10 atm, the gain lifetime in an optically pumped CO₂ active medium is ~ 20 –50 ns.

B. Lasing dynamics in optically pumped CO₂

To validate our findings on small signal gain dynamics of optically pumped CO₂, experiments were performed to study lasing

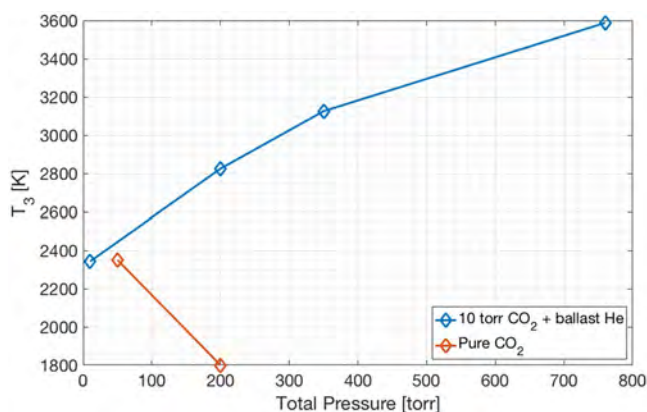


FIG. 8. The peak asymmetric stretching vibrational mode temperature, T_3 , in an optically pumped CO₂ active medium as a function of total pressure for dilute (see the blue curve) CO₂ mixtures and for pure (see the red curve) CO₂.

dynamics and to measure the optical-to-optical conversion efficiency in a similar medium. The experimental setup for these measurements is shown in Fig. 9(a). The cavity of the 10 μm optically pumped CO₂ laser is formed by the dichroic mirror and the 150 g/mm diffraction grating. The optically pumped CO₂ gain medium is contained in a 25 cm long cell with ZnSe windows at the Brewster angle for 10 μm; and the full cavity length is 50 cm. The grating is aligned such that 10.6 μm radiation is reflected directly back into the cavity in a Littrow configuration. The zeroth order reflection of the grating (~10%) was used as an output coupler.

The 40 ns, 4.3 μm Fe:ZnSe laser pulses used to excite the optically pumped CO₂ are measured before and after the CO₂ cell so that absorbed energy can be determined. A HgCdTe detector is used to resolve the temporal profile and measure the energy of the 4.3 μm pump pulse. After propagating through the cell, the 4.3 μm light reflected from the diffraction grating is measured using a calorimeter to determine the absorbed energy. The entire setup is purged with argon to avoid absorption of the 4.3 μm pump pulse in air.

Figure 9(b) shows the measured time evolution of 10 μm lasing in a 35 Torr of pure CO₂ optically pumped at 4.29 μm. A ~120 ns laser pulse was detected ~500 ns after the pump laser pulse. It was found that this delay and the total pulse duration were related to the gain-to-loss ratio within the cavity. Increasing total pressure within the cell reduced gain, resulting in a longer time delay and a longer pulse duration due to the increased number of round-trip passes required to build up a laser pulse.

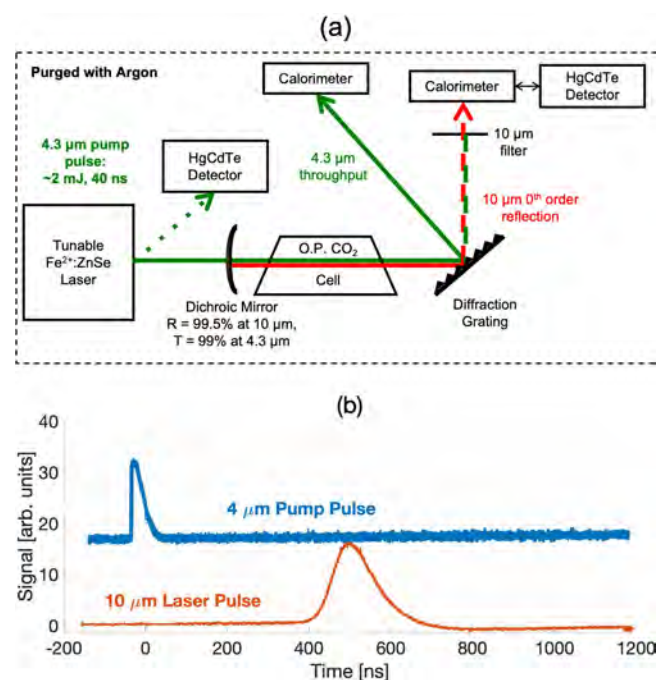


FIG. 9. (a) The experimental setup used to measure lasing in an optically pumped CO₂ active medium. (b) The temporal profiles of the 4.3 μm pump pulse and the 10 μm laser pulse.

These observations demonstrate that the slow relaxation time of the asymmetric stretching mode allows for a continued population inversion on the 10.6 μm lasing transition of interest. The individual rovibrational line of the 001 level is depopulated during lasing, but fast collisional rotational relaxation (τ_{VR}) and vibrational relaxation (τ_{VV}) allow for this state to be very quickly replenished via population from nearby rotational levels and energy stored in the asymmetric stretching mode, respectively. This allows for an efficient extraction of pump energy and demonstrates the importance of reaching high T_3 values.

The results of our study on optical-to-optical conversion efficiency in an optically pumped CO₂ laser are summarized in Fig. 10.

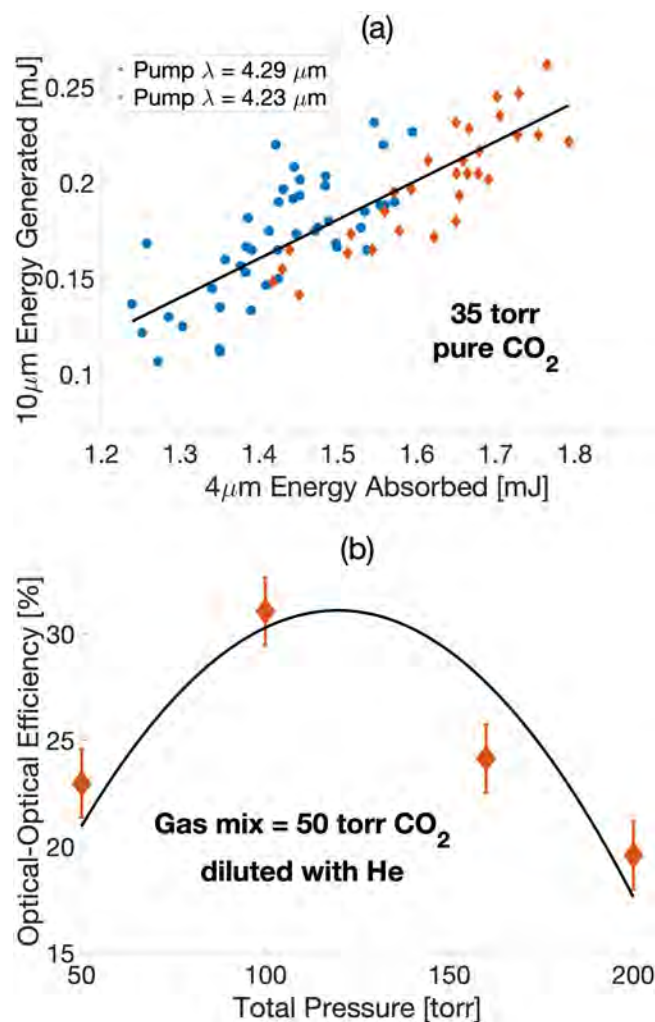


FIG. 10. (a) The amount of 10 μm energy generated in the optically pumped CO₂ laser as a function of absorbed 4.3 μm pump energy. A least squares linear fit to the aggregate data is shown in black. (b) Optical-to-optical conversion efficiency in the optically pumped CO₂ laser for a pump wavelength of 4.23 μm. The black curve indicates a least squares parabolic fit to the data.

Figure 10(a) shows the $10\ \mu\text{m}$ energy generated from lasing in a cell containing 35 Torr of pure CO_2 optically pumped by the Fe:ZnSe laser as described in Sec. III C. Blue dots correspond to lasing output when the pump laser was tuned to $\sim 4.29\ \mu\text{m}$, the peak of the 4P branch of the CO_2 absorption spectrum. Red dots correspond to a pump wavelength of $\sim 4.23\ \mu\text{m}$, the peak of the 4R branch, where absorption is naturally higher, allowing for more efficient pumping. A linear slope can be seen with no indication of pump energy saturation. Figure 10(b) shows the optical-to-optical conversion efficiency of $4.23\ \mu\text{m}$ pump energy to $10.6\ \mu\text{m}$ lasing energy as a function of total pressure in mixtures of 50 Torr of CO_2 and ballast He. A peak conversion efficiency of $>30\%$ was measured, nearing the theoretical quantum limit of $\sim 40\%$.

Using the setup depicted in Fig. 9(a), lasing was not observed at pressures >1 atm. However, by replacing the diffraction grating with a second identical dichroic mirror to maximize the Q-factor of the cavity, lasing was observed at total pressures as high as 3 atm (50 Torr CO_2 diluted with He). At such pressures, the collisional broadening of rovibrational lines resulted in more efficient absorption of the pump energy, and it was, thus, necessary to tune the pump wavelength along the high-J transitions of the 4P absorption branch to $\sim 4.35\ \mu\text{m}$, where absorption is significantly lower. Note that for this high Q-factor cavity (2% output coupling), the $10\ \mu\text{m}$ pulse was observed after a shorter delay of ~ 400 ns. Stable lasing also required a precise tuning of the pump laser wavelength on the line center to avoid resonant nonlinear optical effects in CO_2 as self-focusing and -defocusing of the $4.3\ \mu\text{m}$ pump beam were observed when pumping CO_2 on the red side and the blue side of resonant rovibrational transitions, respectively.²³ It was discovered that both of these effects negatively impacted the efficiency of the optically pumped CO_2 laser and a cylindrical “pencil like” pump beam was optimal.

V. CONCLUSION

In this paper, we presented detailed measurements of kinetics of vibrational temperatures in a CO_2 active medium optically pumped by a $4.3\ \mu\text{m}$ Fe:ZnSe laser. Asymmetric stretching mode vibrational temperature, T_3 , and translational temperature, T_t , are measured as a function of time in optically pumped CO_2 -He mixtures. Peak T_3 values as high as 3600 K are measured in a dilute CO_2 mixture at a total pressure of 1 atm, and gain coefficients of $\sim 30\%/cm$ are seen in 50 Torr of pure CO_2 . Lasing is observed in an optically pumped CO_2 gain medium with an efficiency of $\sim 30\%$ at ~ 100 Torr total pressure, and there is no sign of saturation as $4.3\ \mu\text{m}$ pump energy is increased.

It is calculated that an absorbed energy density of $\sim 1600\ \text{mJ}/\text{cm}^3$ (~ 30 times the energy density available in our experiment) is required to excite a 20 atm gas mixture with a CO_2 partial pressure of 1 atm to a T_3 value approaching 4000 K to be used for efficient sub-picosecond pulse amplification.⁹ The short gain lifetime of the upper laser level, estimated to be ~ 20 – 50 ns at a total pressure of 10 atm, imposes restrictions on the pump laser pulse duration if a high conversion efficiency is to be achieved in a high pressure optically pumped CO_2 amplifier. It should be noted that this time constant may differ depending on experimental conditions and the degree of vibrational excitation that is achieved.

ACKNOWLEDGMENTS

This material is based on work supported by the Air Force Office of Scientific Research under Award No. FA9550-16-1-0139, the Office of Naval Research (ONR) MURI (No. N00014-17-1-2705), and the Department of Energy (DOE) Office of Science Accelerator Stewardship Award No. DE-SC0018378.

DATA AVAILABILITY

The data that support the findings of this study are available from the corresponding author upon reasonable request.

REFERENCES

- 1S. Tochitsky, E. Welch, M. Polyanskiy, I. Pogorelsky, P. Panagiotopoulos, M. Kolesik, E. M. Wright, S. M. Koch, J. V. Maloney, J. Pigeon, and C. Joshi, “Megafilament in air formed by self-guided terawatt long-wavelength infrared laser,” *Nat. Photonics* **13**, 41 (2019).
- 2D. Haberberger, S. Tochitsky, F. Fiuza, C. Gong, R. A. Fonseca, L. O. Silva, W. B. Mori, and C. Joshi, “Collisionless shocks in laser-produced plasma generate monoenergetic high-energy proton beams,” *Nat. Phys.* **8**, 95 (2012).
- 3D. Matteo, J. Pigeon, S. Y. Tochitsky, U. Huttner, M. Kira, S. W. Koch, J. V. Moloney, and C. Joshi, “Control of the nonlinear response of bulk GaAs induced by long-wavelength infrared pulses,” *Opt. Express* **27**, 30462 (2019).
- 4G. Adriukaitis, T. Balčiūnas, S. Ališauskas, A. Pugžlys, A. Baltuška, T. Popmintchev, M. Chen, M.-M. Murnane, and H. C. Kapteyn, “90 GW peak power few-cycle mid-infrared pulses from an optical parametric amplifier,” *Opt. Lett.* **36**, 2755 (2011).
- 5D. Sanchez, M. Hemmer, M. Baudisch, S. L. Cousin, K. Zawilski, P. Schunemann, O. Chalus, C. Simon-Boisson, and J. Biegert, “7 μm , ultrafast, sub-millijoule-level mid-infrared optical parametric chirped pulse amplifier pumped at 2 μm ,” *Optica* **3**(2), 147 (2016).
- 6Y. Yin, A. Chew, X. Ren, J. Li, Y. Wang, Y. Wu, and Z. Chang, “Towards terawatt sub-cycle long-wave infrared pulses via chirped optical parametric amplification and indirect pulse shaping,” *Sci. Rep.* **7**, 45794 (2017).
- 7D. Haberberger, S. Tochitsky, and C. Joshi, “Fifteen terawatt picosecond CO_2 laser system,” *Opt. Express* **18**, 17865 (2010).
- 8M. N. Polyanskiy, I. V. Pogorelsky, and V. Yakimenko, “Picosecond pulse amplification in isotopic CO_2 active medium,” *Opt. Express* **19**, 7717 (2011).
- 9D. Tovey, S. Y. Tochitsky, J. J. Pigeon, G. J. Louwrens, M. N. Polyanskiy, I. Ben-Zvi, and C. Joshi, “Multi-atmosphere picosecond CO_2 amplifier optically pumped at 4.3 μm ,” *Appl. Opt.* **58**, 5756 (2019).
- 10T. Y. Chang and O. R. Wood, “Optically pumped 33-atm CO_2 laser,” *Appl. Phys. Lett.* **23**, 370 (1973).
- 11R. C. Y. Auyeung and J. Reid, “High vibrational temperatures in optically-pumped CO_2 ,” *IEEE J. Quant. Electron.* **24**, 573 (1988).
- 12V. O. Petukhov, S. Y. Tochitsky, and V. V. Churakov, “Investigation of the output parameters of a transversely excited CO_2 laser in the wavelength range 4.2–4.5 μm (10^0 – 10^0 band),” *Sov. J. Quant. Electron.* **20**, 602 (1990).
- 13S. B. Mirov, I. S. Moskalev, S. Vasilyev, V. Smolski, V. V. Fedorov, D. Martyshkin, J. Peppers, M. Mirov, A. Dergachev, and V. Gapontsev, “Frontiers of mid-IR lasers based on transition metal doped chalcogenides,” *IEEE J. Sel. Top. Quant. Electron.* **24**, 1601829 (2018).
- 14W. Wittman, *The CO_2 Laser* (Springer-Verlag, 1987).
- 15K. Siemsen, J. Reid, and C. Dang, “New techniques for determining vibrational temperatures, dissociation, and gain limitations in CW CO_2 lasers,” *IEEE J. Quant. Electron.* **16**, 668 (1980).
- 16I. M. Bertel, V. O. Petukhov, B. I. Stepanov, S. A. Trushin, and V. V. Churakov, “Investigation of the vibrational temperature kinetics in a TEA CO_2 laser,” *Sov. J. Quant. Electron.* **12**, 1044 (1982).
- 17B. F. Gordiets, A. I. Osipov, E. V. Stupochenko, and L. A. Shelepin, “Vibrational relaxation in gases and molecular lasers,” *Sov. Phys. Usp.* **15**, 759 (1973).

- ¹⁸J. T. Yardley and C. B. Moore, "Intramolecular vibration-to-vibration energy transfer in carbon dioxide," *J. Chem. Phys.* **46**, 4491 (1967).
- ¹⁹A. G. Maki, C. C. Chou, K. M. Evenson, L. R. Zink, and J. T. Shy, "Improved molecular constants and frequencies for the CO₂ laser from new high-J regular and hot-band frequency measurements," *J. Mol. Spec.* **167**, 211 (1994).
- ²⁰R. K. Brimacombe and J. Reid, "Measurements of anomalous gain coefficients in transversely excited CO₂ lasers," *IEEE J. Quant Electron.* **19**, 1674 (1983).
- ²¹V. Fedorov, D. Martyshkin, K. Karki, and S. Mirov, "Q-switched and gain-switched Fe:ZnSe lasers tunable over 3.60-5.15 μm ," *Opt. Express* **27**, 13934 (2019).
- ²²A. S. Solodukhin, "Hot-cell-free sequence-band CO₂ laser," *J. Modern Opt.* **34**, 577 (1987).
- ²³J. J. Pigeon, D. Tovey, S. Y. Tochitsky, G. J. Louwrens, I. Ben-Zvi, D. Martyshkin, V. Fedorov, K. Karki, S. Mirov, and C. Joshi, "Resonant nonlinear refraction of 4.3- μm light in CO₂ gas," *Phys. Rev. A* **100**, 011803(R) (2019).